Probing the γ2 Calcium-Binding Site: Studies with γD298,301A Fibrinogen Reveal Changes in the γ294-301 Loop that Alter the Integrity of the "a" Polymerization Site[†,‡]

Michael S. Kostelansky,[§] Karim C. Lounes,[||,⊥] Li Fang Ping,[||] Sarah K. Dickerson,[||] Oleg V. Gorkun,[||] and Susan T. Lord*[,§,||]

Department of Chemistry, University of North Carolina, Chapel Hill, North Carolina 27599, and Department of Pathology and Laboratory Medicine, University of North Carolina, Chapel Hill, North Carolina 27599

Received December 19, 2006; Revised Manuscript Received February 28, 2007

ABSTRACT: To determine the significance of the γ2 calcium-binding site in fibrin polymerization, we synthesized the fibrinogen variant, γD298,301A. We expected these two alanine substitutions to prevent calcium binding in the γ2 site. We examined the influence of calcium on the polymerization of γD298,-301A fibrinogen, evaluated its plasmin susceptibility, and solved 2.7 and 2.4 Å crystal structures of the variant with the peptide ligands Gly-Pro-Arg-Pro-amide (GPRP) and Gly-His-Arg-Pro-amide (GHRP), respectively. We found that thrombin-catalyzed polymerization of γD298,301A fibrinogen was modestly impaired, whereas batroxobin-catalyzed polymerization was significantly impaired relative to normal fibrinogen. Notably, the influence of calcium on polymerization was the same for the variant and for normal fibrinogen. Fibrinogen γD298,301A was more susceptible to plasmin proteolysis in the presence of GPRP. This finding suggests structural changes in the near-by "a" polymerization site. Comparisons of the structures revealed minor conformational changes in the γ294-301 loop that are likely responsible for the weakened "a" site. When considered altogether, the data suggest that the γ2 calcium-binding site does not significantly modulate polymerization. We cannot, however, rule out the possibility that the weakened "a" polymerization site masks an important role for the γ2 calcium-binding site in normal polymerization. Somewhat unexpectedly, the structure data showed that GPRP bound to the "b" site and induced the same local conformational changes as GHRP to this site. This structure shows that "A:b" interactions can occur and suggests that these may participate in normal polymerization.

Fibrinogen, a 340 kDa plasma glycoprotein, plays a key role in blood clotting. The fibrinogen molecule exists as a dimer, and each subunit of the molecule consists of three nonidentical polypeptide chains, Aα, Bβ, and γ. A total of 29 disulfide bonds link the 6 polypeptide chains together, forming an elongated trinodular molecule with structurally distinct regions (*1*, *2*). Generally, fibrinogen's structure can be described as a central E nodule linked to two terminal D nodules by way of coiled-coil connectors (*3*). The amino termini of all six polypeptide chains form the E nodule. Each set of three chains extends out from the E nodule forming the coiled-coil connectors; ultimately the Bβ- and γ-chains fold independently into the β- and γ-modules in the D nodule of the molecule. Within the D nodules, the Aα-chains reverse course, folding back along a section of the coiled-coil region and then extend freely in solution or interact noncovalently with the E nodule (*4*).

The conversion of soluble fibrinogen into an insoluble fibrin clot is initiated by the serine protease thrombin. Thrombin cleaves four fibrinopeptides from the amino termini of the Aα- and Bβ-chains of fibrinogen. Fibrinopeptide A (FpA[1]) cleavage exposes the N-terminal sequence of the α-chains, GPRV, whereas fibrinopeptide B (FpB) cleavage uncovers the N-terminal sequence of the β-chains, GHRP. These new N-terminal residues, called the "A" and "B" knobs, respectively, interact with complementary polymerization pockets, called "a" and "b", located in the γ- and β-modules, respectively (*5*, *6*). The "A:a" and "B:b" interactions occur between fibrin molecules allowing them to spontaneously polymerize into an insoluble fibrin clot.

The current model of polymerization describes the process in two distinct steps, protofibril formation and lateral

[†] This work was supported by National Institutes of Health Grant HL 31048 (to S.T.L.).

[‡] The atomic coordinates have been deposited in the Protein Data Bank (www.rcsb.org) under access codes 2OYI (rfD-γD298,301A+GP) and 2OYH (rfD-γD298,301A+GH).

* Corresponding author. Phone: (919) 966-3548. Fax: (919) 966-6718. E-mail: stl@med.unc.edu.

[§] Department of Chemistry.

[||] Department of Pathology and Laboratory Medicine.

[⊥] Current address: Biolex, Inc., Pittsboro, North Carolina 27312.

[1] Abbreviations: rfD, recombinant fibrinogen fragment D, 1LT9; rfD-BOTH, recombinant fibrinogen fragment D with GPRP and GHRP bound, 1LTJ; rfD-γD298,301A+GP, fragment D of γD298,301A fibrinogen with GPRP bound, 2OYI; rfD-γD298,301A+GH, fragment D of γD298,301A fibrinogen with GHRP bound, 2OYH; rfD-Bβ D398A+GH, fragment D of Bβ D398A fibrinogen with GHRP bound, 1RE3; rfD-GPRVVE, fragment D of recombinant fibrinogen with GPRVVE bound, 2FFD; GPRP, Gly-Pro-Arg-Pro-amide; GHRP, Gly-His-Arg-Pro-amide; AHRP, Ala-His-Arg-Pro-amide; GPRVVE, Gly-Pro-Arg-Val-Val-Glu-amide; FpA, fibrinopeptide A; FpB, fibrinopeptide B; HEPES, 4-(2-hydroxyethyl)-1-piperazineethanesulfonic acid; EDTA, ethylenediaminetetraacetic acid.

10.1021/bi602607a CCC: $37.00
Published on Web 04/06/2007

aggregation. When FpA is cleaved, the subsequent "A:a" interactions between fibrin molecules result in the formation of double-stranded, half-staggered protofibrils, in which two fibrin molecules in one strand are aligned end-to-end by their D nodules, both interacting with the E nodule of a fibrin molecule on the parallel strand (*7*, *8*). Protofibrils grow in length by adding fibrin molecules to each strand. When protofibrils reach a critical size, they begin to associate in the process termed lateral aggregation. This leads to the formation of thick, branching fibrin fibers that form a network called a clot. Subsequent to protofibril formation, FpB is cleaved from fibrin, exposing the "B" polymerization sites, allowing presumed "B:b" interactions to occur. The removal of FpB enhances lateral aggregation; therefore, "B:b" interactions promote this step in polymerization (*9*, *10*). Nevertheless, the fact remains that lateral aggregation can occur in the absence of FpB cleavage (*8*). Thus, other molecular interactions may drive lateral aggregation, but these remain ill defined.

Calcium ions strongly influence fibrinogen function, enhancing polymerization, and modulating fibrinogen's susceptibility to proteolytic enzymes (*11*−*13*). Each D nodule of the fibrinogen molecule possesses four calcium-binding sites that have been identified by X-ray crystallography studies (*14*). Two of the calcium-binding sites reside in the γ-module and the other two in the β-module. The γ1 calcium-binding site is the high-affinity calcium-binding site, located in the γ318-324 loop (*15*, *16*). The β1 calcium-binding site comprises residues in loop β381-385 (*17*). The γ1- and β1-sites are structurally similar because the γ- and β-chain polypeptides are homologous. The β1-site differs from the γ1-site in that it has three calcium-coordinating amino acid residues and one coordinating water molecule, whereas the γ1-site has four calcium-coordinating amino acid residues. The remaining two calcium-binding sites are distinct. The β2 site comprises the side chains of residues Bβ Asp261, Bβ Asp398, and γGlu132 and the backbone carbonyl oxygen of Bβ Asp263 (*14*, *18*−*20*). The β2 calcium-binding site acts as an anchor between the β-module and the coiled-coil connector. Our recent study showed that impairing calcium-binding to the β2 site resulted in increased lateral aggregation, implying that the β2 site modulates lateral aggregation (*20*). Others have suggested that the β2 site impacts the access to the tissue plasminogen activator (tPA)-binding site (*21*). The remaining calcium-binding site, γ2, is located in the loop γ294-301. This site was first identified in crystals where the peptide GHRP, which mimics the B-knob, was bound in the "a" polymerization pocket (*14*). Subsequently, calcium binding to this site was found in one of two conformations in the crystal structure of fragment D from the recombinant variant Bβ D398A fibrinogen with GHRP bound in the "a" pocket (*19*, *20*). The data strongly support the notion that this site is induced by molecular-packing interactions that exist in the crystal form, where the unit cell is $a = 55$ Å, $b = 148$ Å, $c = 230$ Å, and $\alpha = \beta = \gamma = 90$ °. It remains unclear whether the γ2 calcium-binding site is unique to the protein crystal or whether it is present in solution fibrinogen or the fibrin polymer. Moreover, the functional relevance of this site has not been examined.

To determine whether the γ2 calcium-binding site contributes to fibrinogen function, we engineered a variant fibrinogen, γD298,301A, that replaced two aspartic acid residues with alanine. We hypothesized that this double alanine substitution would eliminate the γ2 site. We examined the influence of calcium on the polymerization of γD298,301A fibrinogen, evaluated its plasmin susceptibility, and solved 2.7 and 2.4 Å crystal structures of the variant with the peptide ligands GPRP and GHRP, respectively.

EXPERIMENTAL PROCEDURES

Reagents. All chemicals were of reagent grade and were purchased from Sigma (St. Louis, MO) unless specified otherwise. Human α-thrombin was purchased from Enzyme Research Laboratories, Inc. (South Bend, IN) and batroxobin (*Batroxobin moojeni*) was from CenterChem (Stamford, CT). Plasminogen was purified from human plasma by a method previously described (*22*). Streptokinase was purchased from American Diagnostica (Greenwich, CT). The peptides, GHRP and GPRP, were synthesized as carboxy-amides by the Protein Sequence and Peptide Synthesis Facility at the University of North Carolina at Chapel Hill (Chapel Hill, NC). Cell culture medium with normal recombinant fibrinogen was obtained from the National Cell Culture Center (Minneapolis, MN). Cyanogen bromide-activated Sepharose 4B resin was purchased from Amersham Biosciences (Piscataway, NJ). Monoclonal antibody IF-1 was purchased from Kamiya Biomedical (Seattle, WA).

Synthesis of γD298,301A Fibrinogen. The expression vector, pMLP-γ, includes the cDNA of the human fibrinogen γ-chain and has been described previously (*23*). Aspartic acid residues at positions γ298 and γ301 were substituted with alanine residues by oligo-directed mutagenesis, using the Transformer site-directed mutagenesis kit (Clontech, Palo Alto, CA) (*24*). The mutagenic primer was 5′GGCTTTGATTTTGGCGATGCTCCTAGTGCCAAGTTTTTCACATCC3′. The mutated cDNA was sequenced to ensure that only the intended changes were made. Synthesis of γD298,301A fibrinogen was carried out as described (*25*). Briefly, the altered pMLP-γ vector and the pMSV-His selection vector were cotransfected into Chinese hamster ovary cells (CHO cells) expressing the Aα- and Bβ-polypeptide chains of human fibrinogen. An enzyme-linked immunosorbent assay was utilized to screen single clones, and those expressing the most fibrinogen were used for large-scale protein expression. Protein production was performed in roller bottles using serum-free medium containing aprotinin. The medium was harvested periodically to collect the secreted fibrinogen. Phenylmethylsulfonyl fluoride was added (0.1 mM) and the medium stored at −20 °C.

Purification of Recombinant Fibrinogen. Both normal and γD298,301A fibrinogens were purified from the medium by a two-step method outlined previously (*26*). Briefly, proteins were precipitated from the medium with ammonium sulfate, and fibrinogen was isolated from the precipitate by immunoaffinity chromatography with the calcium-dependent, fibrinogen-specific antibody, IF-1, eluting the bound protein with buffer containing 5 mM EDTA. Purified fibrinogen was dialyzed against 20 mM HEPES at pH 7.4 and 150 mM NaCl (HBS) with 1 mM $CaCl_2$ followed by extensive dialysis against HBS. Aliquots of purified protein were stored at −70 °C. Reduced and nonreduced samples of the purified recombinant fibrinogens were subject to SDS−PAGE analysis to confirm purity and proper polypeptide chain composition of the protein.

Fibrinopeptide Release. Fibrinopeptide release was measured as previously described (*25*, *27*). Briefly, 0.1 mg/mL fibrinogen in HBS was treated with 0.005 U/mL human α-thrombin at ambient temperature. Reactions were stopped by boiling at specified time points, centrifuged, and the supernatants were analyzed by reverse-phase HPLC to quantify the FpA and FpB released. The data were analyzed for statistical significance using an unpaired *t*-test. Values were considered significant for $p < 0.05$.

Fibrinogen Polymerization. Thrombin- or batroxobin-catalyzed polymerization of normal and γD298,301A fibrinogen was monitored by measuring the rise in turbidity at 350 nm in a SpectraMax-340PC Microplate reader (Molecular Devices, Sunnyvale, CA) as described previously (*28*). The polymerization reactions were carried out at ambient temperature in HBS buffer containing 0.01, 1, or 10 mM $CaCl_2$. The chloride ion concentration was held constant in each reaction by adjusting the NaCl concentration. All fibrinogen samples were subject to overnight dialysis against HBS containing 0.01 mM $CaCl_2$, and the final calcium concentration was adjusted 30 min before polymerization. Dilution of thrombin in HBS was done immediately before use. Reactions were initiated by adding 10 μL of enzyme (1 U/mL of thrombin or 1 BU/mL of batroxobin) with a multichannel pipetter to wells containing 90 μL of fibrinogen (0.2 mg/mL). Upon the addition of enzyme, the wells were mixed for 5 s using the automix function of the instrument, and the absorbance was read every 24 s for 3 h. A minimum of three experiments in duplicate were carried out for each calcium concentration. Polymerization data were assessed to determine the lag time, V_{max}, and final absorbance (clot absorbance at 350 nm at 80 min) for each reaction as described previously (*29*) and compared to determine statistical significance using a *t*-test. A difference was considered significant for $p < 0.05$.

Plasmin-Protection Assay. Plasmin was prepared by activating 100 μg/mL plasminogen with 100 U/mL streptokinase for 40 min at 37 °C. Normal recombinant and γD298,301A fibrinogens (0.2 mg/mL) in HBS were digested by incubating with 10 μg/mL plasmin for 4 h at 37 °C. The digests were carried out under several conditions that included 0.01 mM or 0.1 mM $CaCl_2$, 5 mM EDTA, or varying concentrations of the peptides GPRP or GHRP with 1 mM EDTA or $CaCl_2$ present. The digest reactions were stopped by heating the sample at 100 °C for 5 min, and analyzed on 7.5% SDS−PAGE gels, under non-reducing conditions.

Preparation of Fragment D from γD298,301A fibrinogen. Eight milligrams of γD298,301A fibrinogen (final concentration of 0.61 mg/mL) in HBS with 20 mM $CaCl_2$ was used to produce fragment D (rfD-γD298,301A), as described previously (*18*). Briefly, the reaction was initiated by adding 100 μL of immobilized TPCK Trypsin (Pierce, Rockford, IL). Digestion at room temperature was carried out over a 4 day period, and the progress of the digest was monitored by SDS−PAGE. When only rfD-γD298,301A and fragment E bands were visible by SDS−PAGE (data not shown), the digest was stopped by removing the trypsin-coated beads by filtering through a 0.22 μm syringe fitting filter (Costar, Corning, NY). The resulting digested protein was stored at −70 °C.

Fragment D of γD298,301A fibrinogen was purified by lectin affinity chromatography based on a method described by Solis et al. (*30*). Briefly, the entire amount (8 mg) of digested γD298,301A fibrinogen was loaded onto a 4 mL Concanavalin A agarose affinity column equilibrated with 10 mM Tris at pH 7.4 and 1 M NaCl (loading buffer) at a flow rate of 10 mL/h. The column functioned by binding fragment E while allowing fragment D to flow through the column. The flowthrough was kept, and extensive washing with loading buffer was employed to recover fragment D. Unwanted fragment E was eluted from the column using loading buffer containing 0.1 M α-methyl-D-glucopyranoside. The flowthrough containing rfD-γD298,301A was dialyzed against 50 mM Tris at pH 7.4 and concentrated with a centrifugal filter device (50 kDa MW cutoff, Millipore Corp., Billerica, MA) and stored at 4 °C.

Crystallization of γD298,301A Recombinant Fragment D. Crystals of rfD-γD298,301A were grown by sitting-drop vapor diffusion at 4 °C in the presence of a peptide ligand, GPRP or GHRP. Conditions were screened close to those previously determined for other fibrinogen fragment D crystals (*14*−*20*). For rfD-γD298,301A crystals, sitting drops containing 5 μL of 10 mg/mL protein in HBS with 3 mM GPRP or GHRP were mixed with an identical volume of well solution containing 50 mM Tris at pH 8.5, 2 mM NaN_3, 12.5 mM $CaCl_2$, and 11% PEG 3350. Seeding from crystals of normal rfD was employed to maximize the growth of the γD298,301A fragment D crystals. Diffraction quality crystals grew in a few days time. Crystals were cryoprotected for low-temperature data collection by dipping in a solution containing the crystallant plus 20% glycerol.

X-ray Data Collection. Diffraction data for the rfD-γD298,301A+GP crystal were collected at 100 K with a Rigaku RUH3R rotating anode generator with Osmic confocal blue multilayer optics and a Rigaku R-AXIS IV^{2+} detector at the University of North Carolina at Chapel Hill. The data for the rfD-γD298,301A+GH crystal were collected at 100 K at the SER-CAT beamline 22-ID of the Advanced Photon Source. X-ray diffraction data were processed with DENZO and SCALEPACK (*31*).

Structure Determination. The unit cell dimensions of the rfD-γD298,301A+GP and rfD-γD298,301A+GH crystals (Table 1) were isomorphous to those of normal recombinant fragment D with GPRP and GHRP bound (rfD-BOTH, pdb code 1LTJ). Thus, rfD-γD298,301A+GP and rfD-γD298,-301A+GH were refined by rigid-body minimization followed by simulated annealing using the 1LTJ structure as a starting model. Alanine residues were substituted for the aspartic acid residues at positions γ298 and γ301 in the starting model, and CNS (*32*) was utilized for the refinement.

Before refinement, 5% of the observed data was set aside for cross-validation using the free *R*-factor statistic (*33*). After the initial round of refinement, manual fitting was performed on both structures using the software program O (*34*) and σA-weighted $|2F_o - F_c|$ and $|F_o - F_c|$ electron density maps (*35*). After manual fitting, the structures were further refined using CNS. The refinement protocol used least-squares minimization, simulated annealing, and individual temperature factor refinement including an overall anisotropic *B*-factor and bulk solvent correction. Cycles of manual fitting and refinement were carried out while following the working *R*-factor and free *R*-factor statistics to evaluate the rebuilding

Table 1: X-ray Crystallography Data

	rfD-γD298,301A+GH	rfD-γD298,301A+GP
	data collection	
resolution (Å)	50−2.4	50−2.7
wavelength (Å)	1.0000	1.5418
space group	$P2_12_12_1$	$P2_12_12_1$
cell constants (Å)	$a = 89.2$	$a = 89.0$
	$b = 94.1$	$b = 94.0$
	$c = 226.7$	$c = 226.4$
	$\alpha = \beta = \gamma = 90^0$	$\alpha = \beta = \gamma = 90^0$
total observations	404,998	245,178
unique reflections	71,647	52,450
mean redundancy	5.7	4.7
R_{sym}[a] (%; highest shell)	9.1 (46.5)	11.6 (48.4)
completeness (%; highest shell)	96.0 (81.6)	98.3 (99.8)
mean I/σ (highest shell)	15.4 (1.9)	13.1 (3.3)
	refinement	
resolution range (Å)	18−2.4	18−2.7
molecules/asymmetric unit	2	2
R_{cryst}[b] (%)	22.0	21.6
R_{free}[c] (%)	25.9	25.6
RMSD bond lengths (Å)	0.0062	0.0065
RMSD bond angles (^{0})	1.23	1.26
average *B*-factor	46.4	41.3
number of model atoms	10,853	10,790
number of solvent sites	239	150

[a] $R_{sym} = \Sigma|I - \langle I\rangle|$, where I is the observed intensity, and $\langle I\rangle$ is the average intensity of multiple symmetry-related observations of that reflection. [b] $R_{cryst} = \Sigma||F_o| - |F_c||/\Sigma|F_o|$, where F_o and F_c are the observed and calculated structure factors, respectively. [c] $R_{free} = \Sigma||F_o| - |F_c||/\Sigma|F_o|$ for 5% of the data withheld from structural refinement.

progress. In the final step of the modeling process, 150 and 239 water molecules were added to the structures of rfD-γD298,301A+GP and rfD-γD298,301A+GH, respectively. In addition, cis peptide bonds were modeled at positions Bβ407 and γ339. The working *R*-factor, 23.4%, and the free *R*-factor, 27.5%, for the rfD-γD298,301A+GP structure dropped to 21.6% and 25.6%, respectively. Likewise, the working *R*-factor decreased from 23.9% to 22.0%, and the free *R*-factor dropped from 27.7% to 25.9% in the rfD-γD298,301A+GH structure after the appropriate changes were introduced.

RESULTS

Characterization of γD298,301A Fibrinogen. We synthesized γD298,301A fibrinogen in CHO cells and purified it from the cell culture medium as outlined in the Experimental Procedures section. SDS−PAGE analysis showed that the variant protein assembled into a 340 kDa molecule similar to normal recombinant fibrinogen and consisted of the three expected polypeptide chains that compose fibrinogen (data not shown). As with other variant fibrinogens with altered Asp residues in the γ-chain, the γ-chain of γD298,301A fibrinogen had an increased mobility relative to the γ-chain of normal fibrinogen. The gels also showed that the recombinant proteins were pure and homogeneous.

Fibrinopeptide Release. We examined thrombin-catalyzed fibrinopeptide release for normal and γD298,301A fibrinogens by measuring the percent of released fibrinopeptides at specific time points (data not shown). The specificity constant (k_{cat}/K_m, ± SD) for FpA was 6.6 ± 0.5 ($\times 10^6 M^{-1}$ s^{-1}) for normal fibrinogen and 5.7 ± 0.5 ($\times 10^6 M^{-1}$ s^{-1}) for γD298,301A fibrinogen; the specificity constant for FpB was 3.1 ± 0.5 ($\times 10^6 M^{-1}$ s^{-1}) and 0.9 ± 0.1 ($\times 10^6 M^{-1}$ s^{-1}) for normal and γD298,301A fibrinogen, respectively. Statistical analysis utilizing an unpaired *t*-test showed that the specificity constants for FpA release were similar ($p > 0.05$), indicating that the variant fibrinogen is a normal thrombin substrate. In contrast, the specificity constants for FpB release were different ($p < 0.05$). Previous studies have shown that the kinetics of FpB release depend on the formation of protofibrils (*36*, *37*); therefore, the slower release of FpB indicates that the protofibril formation of γD298,301A fibrinogen is impaired. A kinetic model of fibrin polymerization shows that changes in the rate of protofibril growth do not affect the lag time measured by turbidity (*38*). We concluded that the slower release of FpB indicates that protofibril growth is impaired in this variant fibrinogen.

Fibrin Polymerization. We examined the thrombin-catalyzed polymerization of normal and γD298,301A fibrinogen at 0.01, 1, and 10 mM $CaCl_2$ by monitoring the change in turbidity at 350 nm and determining values for the lag time, V_{max}, and final absorbance. The lag time corresponds to the rate of protofibril formation, whereas V_{max} indicates the maximum rate of lateral aggregation, and final absorbance denotes the final fiber thickness. Representative polymerization curves are shown in Figure 1A, and the averaged parameters are summarized in Table 2. Although there were differences between the variant and normal polymerization profiles, these were modest. Only at 1 mM $CaCl_2$ were all three parameters significantly different from the normal. Furthermore, the overall effect of calcium concentration was similar for the normal and the variant fibrinogens; polymerization was enhanced by increasing calcium concentration with a shorter lag time, a faster V_{max}, and a higher final absorbance.

Polymerization experiments were also performed with batroxobin, which cleaves only FpA. Representative data are shown in Figure 1B, and polymerization parameters are presented in Table 3. Batroxobin-catalyzed polymerization of γD298,301A fibrinogen was impaired at all calcium concentrations, and most differences were statistically significant compared to the normal. The lag times were all about 2-fold longer than that of the normal. The V_{max} values were reduced, although the magnitude of the differences varied with calcium concentration; at 0.01 mM $CaCl_2$, V_{max} for γD298,301A was only 30% of that of the normal, whereas at 1 mM and 10 mM $CaCl_2$, V_{max} was about 60% of that of the normal. The final absorbance for γD298,301A fibrinogen was lower than that for normal fibrinogen, although the magnitude of this difference varied with calcium concentration, the variant was 45% of that of the normal at 0.01 mM $CaCl_2$, 70% at 1 mM $CaCl_2$, and 80% at 10 mM $CaCl_2$. Overall, increased calcium concentrations affected γD298,-301A polymerization, in a fashion similar to that of normal fibrinogen, by reducing lag time, increasing V_{max}, and augmenting final absorbance. Thus, batroxobin-catalyzed polymerization of the variant was impaired relative to that of the normal but showed a calcium dependence that was similar to that of the normal.

A comparison of thrombin-catalyzed to batroxobin-catalyzed polymerization shows notable differences. With both enzymes at all calcium concentrations, the lag times

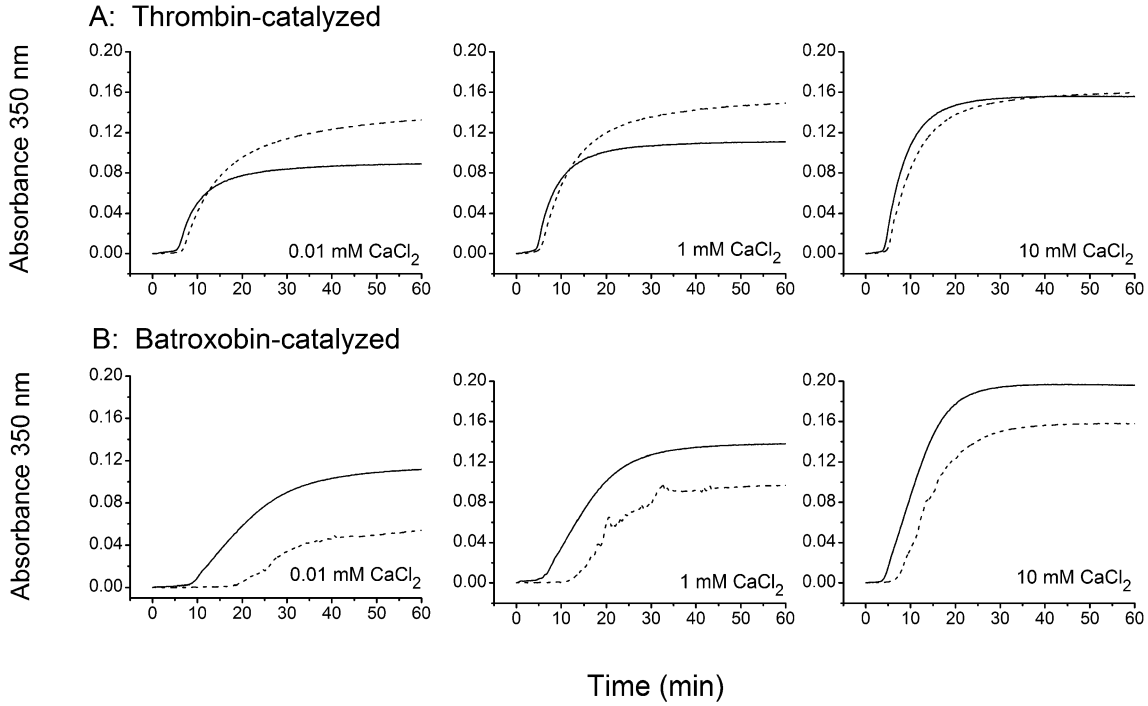

FIGURE 1: Representative turbidity curves. The polymerization of normal (—) and γD298A,D301A (---) fibrinogen catalyzed by thrombin (A) and batroxobin (B) at 0.01, 1, and 10 mM $CaCl_2$ with a constant chloride ion concentration (150 mM) is shown.

Table 2: Thrombin-Catalyzed Polymerization Parameters (Mean ± 1 SD, $n = 3$) of Normal and γD298,301A Fibrinogens[a]

	lag time (10^2 s)	V_{max} (10^{-4} s^{-1})	final ABS
	normal		
0.01 mM $CaCl_2$	3.3 ± 0.3	2.1 ± 0.4	0.09 ± 0.01
1 mM $CaCl_2$	2.6 ± 0.2	3.0 ± 0.4	0.11 ± 0.01
10 mM $CaCl_2$	2.4 ± 0.2	3.9 ± 0.7	0.15 ± 0.01
	γD298,301A		
0.01 mM $CaCl_2$	3.9 ± 0.7	2.0 ± 0.4	0.13 ± 0.1
1 mM $CaCl_2$	*3.3 ± 0.4	*2.3 ± 0.4	*0.15 ± 0.01
10 mM $CaCl_2$	*2.9 ± 0.1	3.1 ± 0.5	0.17 ± 0.01

[a] The parameters lag time, V_{max}, and final ABS were defined in the Experimental Procedures section. A *t*-test was used to compare the lag time, V_{max}, and final ABS of the normal and γD298,301A fibrinogens at each calcium concentration. A difference was determined as statistically significant (*) at p values <0.05.

Table 3: Batroxobin-Catalyzed Polymerization Parameters (Mean ± 1 SD, $n = 3$) of Normal and γD298,301A Fibrinogens[a]

	lag time (10^2 s)	V_{max} (10^{-4} s^{-1})	final ABS‡
	normal		
0.01 mM $CaCl_2$	4.7 ± 0.2	0.96 ± 0.13	0.11 ± 0.01
1 mM $CaCl_2$	2.8 ± 0.6	1.4 ± 0.1	0.13 ± 0.01
10 mM $CaCl_2$	2.2 ± 0.1	2.5 ± 0.6	0.17 ± 0.02
	γD298,301A		
0.01 mM $CaCl_2$	*10.4 ± 0.8	*0.30 ± 0.14	*0.05 ± 0.01
1 mM $CaCl_2$	*7.2 ± 0.4	*0.88 ± 0.22	*0.09 ± 0.01
10 mM $CaCl_2$	*3.9 ± 0.1	1.5 ± 0.4	0.14 ± 0.02

[a] A *t*-test was used to compare the lag time, V_{max}, and final ABS of normal and γD298,301A fibrinogens at each calcium concentration. A difference was determined as statistically significant (*) at p values <0.05.

for γD298,301A fibrinogen were longer than that of the normal, but the magnitudes of these increases were quite different: 1.2- to 1.3-fold for thrombin and 1.8- to 2.6-fold for batroxobin. When comparing V_{max} values with thrombin, there was little or no difference between the variant and the normal. In contrast, V_{max} values with batroxobin were different, in particular at the lowest calcium concentration, where the rate for the variant was about a third that of normal. The most obvious difference was seen in the final absorbance for γD298,301A fibrinogen, as this was higher than that of the normal in thrombin-catalyzed reactions and lower than that of the normal in batroxobin-catalyzed reactions. These differences indicate that the release of FpB from γD298,-301A fibrinogen affected polymerization in a manner different from the release of FpB from normal fibrinogen.

Plasmin Protection. To further characterize the "a" polymerization site of γD298,301A fibrinogen, we performed plasmin protection assays. In this experiment, the addition of GPRP or calcium to the reaction limits the plasmin proteolysis of fibrinogen to fragment D_1. In the presence of EDTA or in the absence of GPRP, fragment D_1 is further cleaved to the smaller fragments D_2 and D_3. We found that plasmin proteolysis of γD298,301A fibrinogen was not limited with 2 mM GPRP, a concentration that fully protected normal fibrinogen (data not shown). With increasing concentrations of GPRP, above 5 mM, limited cleavage of γD298,301A was apparent, and even at the highest peptide concentration, that is, 20 mM, significant levels of fragments D_2 and D_3 remained (data not shown).

To determine whether the addition of calcium with the peptide would increase plasmin protection, we examined the effect of adding calcium in the presence of 5 mM GPRP. The data are shown in Figure 2. For normal fibrinogen, plasmin protection was essentially complete at all calcium concentrations in the absence of the peptide such that the addition of the peptide had little or no consequence. In contrast, samples with 0.01 mM calcium in the absence of the peptide showed only partial protection in plasmin digests of γD298,301A fibrinogen; here, the addition of the peptide increased protection, although in an incomplete manner. With higher calcium concentration, we observed increased protec-

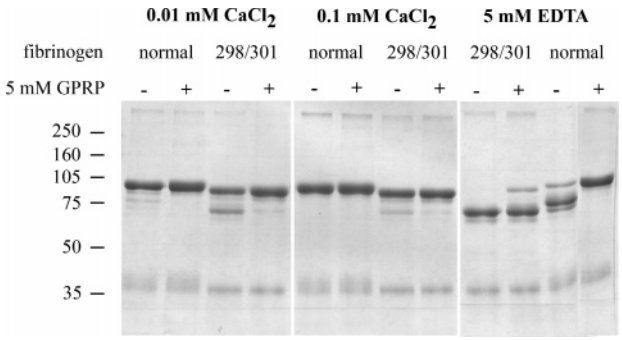

FIGURE 2: Plasmin protection assays. Plasmin digests of normal and γD298,301A fibrinogen with and without 5 mM GPRP with 0.01 or 0.1 mM $CaCl_2$ or 5 mM EDTA. Samples were incubated for 4 h, run on 7.5% SDS−PAGE, and stained with Coomassie blue, as described in the Experimental Procedures section. Note that samples with EDTA are shown with the variant fibrinogen to the left of the normal.

tion that was further enhanced by the addition of 5 mM peptide. These observations are consistent with the conclusion that the two alanine substitutions altered both peptide binding to the "a" site and calcium binding.

We also examined whether GHRP could induce protection from plasmin in normal or γD298,301A fibrinogen. Under conditions of increasing concentrations of GHRP, up to 20 mM, the variant and normal fibrinogens both showed little protection from plasmin, with digest patterns similar to those seen with EDTA (data not shown). These data suggest that GHRP binding to the "b" site, or the "a" site, as indicated in the structure data described previously and herein, does not influence plasmin cleavage.

Structure of rfD-γD298,301A. We solved 2.7 and 2.4 Å X-ray crystal structures of fragment D of γD298,301A in the presence of GPRP (rfD-γD298,301A+GP) and GHRP (rfD-γD298,301A+GH), respectively. We were not able to obtain crystals of the variant fragment in the absence of the peptide. The aspartic acid to alanine substitutions were clearly evident in electron density maps of both structures. When the rfD-γD298,301A+GP structure is aligned by Cα-atoms with the structure of the D fragment from normal recombinant fibrinogen crystallized in the presence of GPRP and GHRP (rfD-BOTH, 1LTJ), the RMSD = 0.32 Å. Similarly, the Cα-atom alignment of the rfD-γD298,301A+GH with rfD-BOTH gives an RMSD of 0.26 Å. These low rmsd values demonstrate that the global structure of the D nodule of γD298,301A is similar to normal fibrinogen.

A detailed inspection of the rfD-γD298,301A+GP and rfD-γD298,301A+GH structures aligned with rfD-BOTH revealed subtle movement of the loop γ294−301. In particular, the loop in rfD-γD298,301+GP is obviously different from the loop in rfD-BOTH. As shown in Figure 3, the variant structures are well aligned with the normal at residues γ293 and γ302, but the loops connecting these residues differ. Figure 3B depicts a critical hydrogen bond between the Cα backbone nitrogen of residue γG296 and a side chain oxygen of residues γD301. This hydrogen bond is found in the presence and absence of calcium in the γ2 site. In γD298,301A fibrinogen, the elimination of the aspartic acid side chain at position 301 removes the possibility of this hydrogen-bond interaction and results in the observed conformational flexibility of the γ294−301 loop.

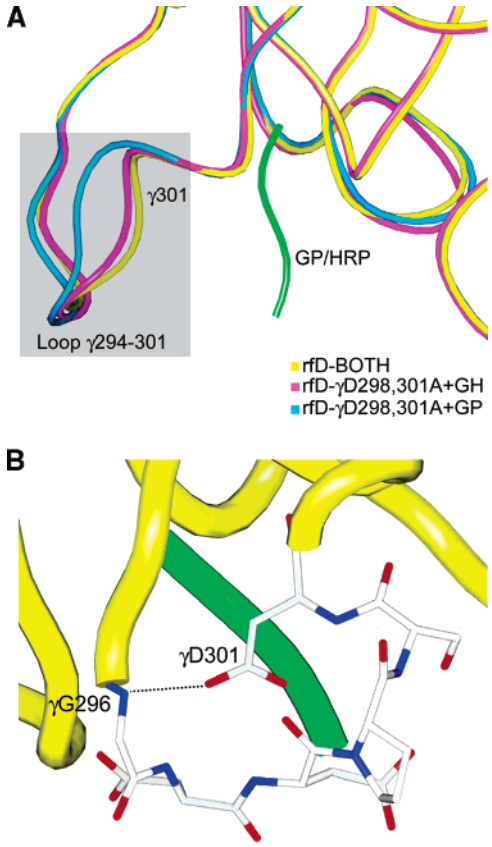

FIGURE 3: Illustration of the flexibility of loop γ294−301 in γD298,301A. (A) The image was generated after aligning the Cα atoms of rfD-γD298,301A+GH (pink) and rfD-γD298,301A+GP (blue) with normal rfD-BOTH (1LTJ, yellow). The RMSD from the alignment of rfD-γD298,301A+GH with rfD-BOTH was 0.26 Å, whereas the RMSD of the rfD-γD298,301A+GP/rfD-BOTH alignment was 0.32 Å. The green worm represents the approximate location of either GPRP or GHRP bound to the "a" polymerization site in the structures. Notice that the conformation of loop γ294−301 appears most altered in the γ D298,301A+GP structure. (B) Depiction of a crucial hydrogen-bond interaction in loop γ294−301 of normal recombinant fibrinogen. The structure of normal rfD-BOTH (1LTJ) is shown as a yellow worm, GPRP bound in the "a" polymerization site is shown as a green worm, and residues γ296−301 are shown as sticks. Note the hydrogen-bond interaction between the side chain of γD301 and the backbone nitrogen of γG296 that is conserved with or without calcium bound in the γ2 site in normal fibrinogen. This hydrogen bond is eliminated by the mutation to alanine.

In the rfD-γD298,301A+GH structure, the peptide GHRP was present in both the "a" and "b" polymerization sites, as expected from previous structures of fibrinogen fragment D crystals grown in the presence of only GHRP (*14*, *20*). The conformation of the peptide bound in the "a" polymerization site, however, was unexpected. Previously, GHRP bound in the "a" polymerization site has been seen in two crystal forms. In the form with unit cell dimensions of $a = 89$ Å, $b = 94$ Å, and $c = 227$ Å, (Figure 4A) calcium is not present in the γ2 site, whereas in the form with unit cell dimensions of $a = 55$ Å, $b = 148$ Å, and $c = 230$ Å (Figure 4B), calcium is present in the γ2 site. Comparing the structures of bound peptides in these two crystal forms shows that they differ in the orientation of the histidine side chain; it points toward the solvent in the first crystal form and into the pocket in the second. The rfD-γD298,301A+GH structure showed the histidine side chain pointed into the pocket (Figure 4C) for both molecules in the asymmetric unit, even though this

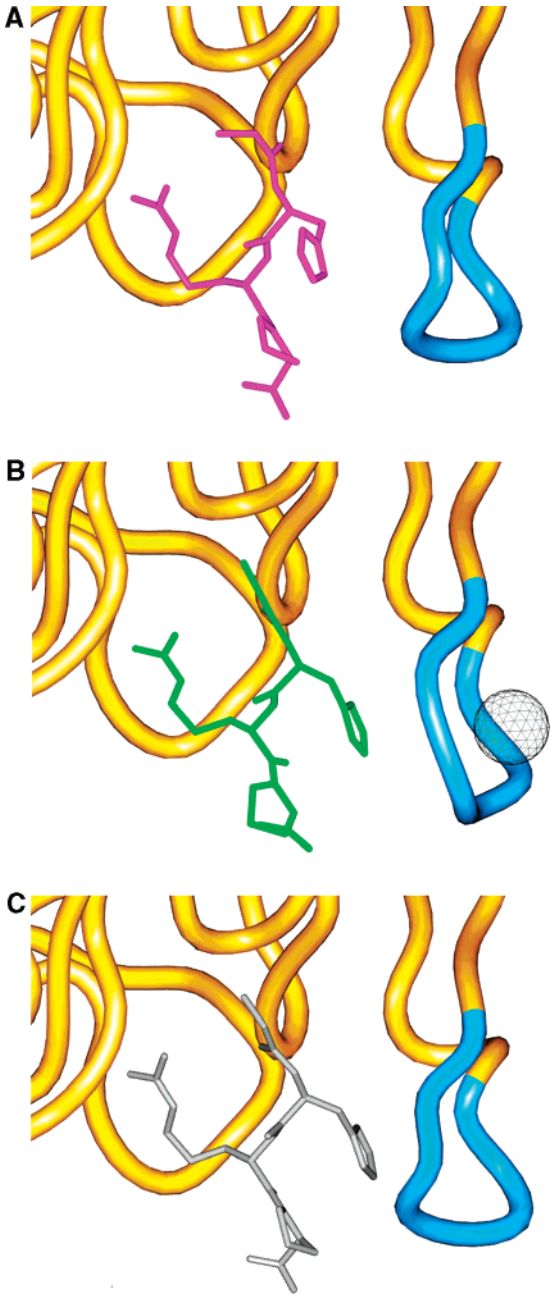

FIGURE 4: Conformation of GHRP in the "a" polymerization site. (A) Conformation of GHRP bound to fragment D in the crystal form lacking the γ2 calcium-binding site (rfD-γE132D+GH, 1RF1). (B) Conformation of GHRP bound to fragment D in the crystal form with calcium present in the γ2 site (rfD-BβD398A+GH, 1RE3). (C) GHRP bound to rfD-γD298,301A+GH; here, the crystal form is that seen in A, with no bound calcium, but the conformation of bound GHRP is similar to that seen in B.

crystal has unit cell dimensions of $a = 89$ Å, $b = 94$ Å, and $c = 227$ Å and no calcium in the γ2 site. We conclude that the subtle movement of the loop γ294−301 is associated with a small increase in volume of the "a" polymerization site such that the histidine side chain is accommodated within the binding pocket even in this more common crystal form.

In the rfD-γD298,301A+GP structure, the peptide GPRP was bound not only in the "a" polymerization site, as expected, but also in the "b" polymerization site, as clearly shown in the difference electron density map (Figure 5). The structure of the "b" polymerization site with GPRP in rfD-γD298,301A+GP is in good agreement with that of the "b"

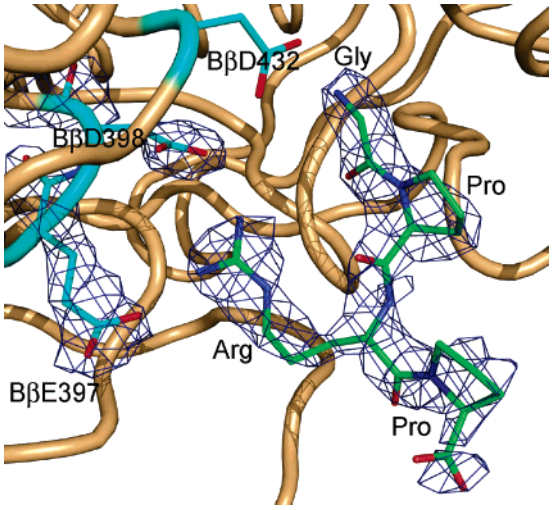

FIGURE 5: Difference in electron density in the "b" polymerization site. The $|F_o - F_c|$ electron density map was contoured at 3.0 σ for a model that excluded the presence of the peptide in the "b" polymerization site as well as the native positions for residues BβE397 and BβD398. The data demonstrate that GPRP is present in the "b" polymerization site with the concurrent flip of residues BβE397 and BβD398 toward the peptide. Although not shown here, the binding event eliminated the β2 calcium-binding site.

polymerization site with GHRP in rfD-BOTH. With GPRP binding to the "b" polymerization site, the side chains of residues BβE397 and BβD398 point toward the bound peptide interacting with the arginine side chain in the same manner as that seen with GHRP bound to this site. In addition, no calcium was present in the β2 site, and a salt link was seen between residues γE132 and αK157. We conclude that under the conditions of crystallization, both GPRP and GHRP are able to bind in both polymerization pockets.

DISCUSSION

Our laboratory has used the analysis of engineered fibrinogen variants to further define the molecular mechanisms that mediate the conversion of fibrinogen to fibrin. We have recently focused on the role of the D-domain, where we can complement biochemical data with atomic resolution crystal structures. The data, especially the structural data, have proved invaluable in understanding the consequences of introducing engineered changes in fibrinogen. We have synthesized variants within polymerization sites "a", "b", and all four calcium-binding sites, γ1, γ2, β1, and β2. Here, we report an analysis of the variant fibrinogen, γD298,301A, with substitutions introduced to disrupt calcium binding to the γ2 site.

Crystal structures of fragment D in the presence of either GPRP or GHRP showed that the two substituted alanine residues induced only local changes in the structure of the D-domain, limited to the γ294−301 loop. Calcium was not present in the γ2 site as expected for this crystal form with unit cell dimensions of $a = 89$ Å, $b = 94$ Å, and $c = 227$ Å. Our results, therefore, do not address whether these substitutions would impair calcium binding to this site in the alternate crystal form, $a = 55$ Å, $b = 148$ Å, $c = 230$ Å, and $\alpha = \beta = \gamma = 90$ °, where the γ2 site was identified (*19*, *20*). Nevertheless, we propose that calcium binding to the γ2 site is impaired in γD298,301A fibrinogen because

other variants with single substitutions at side chains critical to calcium coordination have impaired, if not eliminated, calcium binding to the γ1 and β2 sites (*19*, *20*, *39*). The structures also showed that when either peptide is bound in the "b" polymerization site in rfD-γD298,301A, the β2 calcium-binding site was not occupied. We interpret our biochemical data within the context of these structures, although they have been obtained at a calcium concentration (12.5 mM) that is higher than that used for the biochemical analyses.

We found that thrombin-catalyzed polymerization of γD298,301A fibrinogen differed modestly from normal polymerization. Nevertheless, the delayed release of FpB, which has been similarly observed for other variants with impaired protofibril formation, suggests that protofibril formation is indeed impaired. Of note, the small differences between the variant and normal polymerization were similar at all calcium concentrations, that is, the effect of calcium on the polymerization of the variant paralleled the effect of calcium on the polymerization of normal fibrinogen. This calcium effect contrasts markedly with the effect of calcium on the polymerization of the β2 site variant, γE132A fibrinogen (*19*, *20*). With γE132A fibrinogen, the final absorbance was highest at the lowest calcium concentration and decreased with increasing calcium, exactly the opposite of the calcium dependence of final absorbance for normal fibrinogen. We concluded, and others concur, that the β2 calcium-binding site has a modulating role in polymerization (*18*, *20*, *21*). In contrast, the current data suggest that calcium binding to the γ2 site has little or no role in normal polymerization. Because the mutations, which were intended to disrupt calcium binding to the γ2 site, also altered the "a" polymerization site, we have not been able to independently assess the role of the γ2 site. Unequivocal measurement of the role of the γ2 site will require the examination of a fibrinogen variant where only γ2 calcium binding is impaired.

It is also noteworthy that the modestly impaired polymerization of γD298,301A fibrinogen contrasts with the significantly impaired polymerization of variants with substitutions in single residues that coordinate calcium binding in the γ1 site. These substitutions, γD318A or γD320A, severely impaired both protofibril formation and lateral aggregation. In comparison, the loss of the γ2 calcium-binding site has a more subtle role in polymerization, likely due to subtle structural changes in the "a" polymerization site. We concluded that it is the loss of calcium binding at this site and the conformational flexibility of the γ294−301 loop that caused the impaired polymerization.

The plasmin protection experiments are consistent with the conclusion that the "a" polymerization site is altered. In the presence of EDTA, GPRP binding to γD298,301A fibrinogen was markedly reduced. Moreover, the addition of calcium, even as low as 0.01 mM, enhanced GPRP binding. These results suggest that the polymerization of γD298,301A is close to that of the normal because calcium binding to the γ1 site facilitates "A:a" interactions. We believe that the calcium in the γ1 site stabilizes the structure of this binding pocket. Furthermore, because the simultaneous substitutions of γD298 and γD301 to alanine modestly weakened the "A:a" interactions, the experiments did not measure the true contribution of the γ2 site to polymerization.

The comparison of thrombin-catalyzed to batroxobin-catalyzed polymerizations further supports this conclusion. If the "A:a" interactions are weakened, then polymerization mediated by either enzyme should be close to that of the normal, as observed. Moreover, one would anticipate that batroxobin-catalyzed polymerization would be more impaired than thrombin-catalyzed polymerization because the weak "A:a" interactions would be more apparent without "B:b" interactions, as shown by our data.

In the rfD-γD298,301A+GP structure, we were surprised that the electron density maps revealed GPRP bound to the "b" polymerization site. This observation is contrary to previous crystallographic studies reporting GPRP bound exclusively to the "a" polymerization site (*16*). The structure of GPRP in the "b" polymerization site in the variant fragment D was quite analogous to GHRP bound to the "b" site of normal fragment D. The observation that GPRP can bind to both the "a" and "b" polymerization sites is consistent with earlier biochemical studies that suggested GPRP could bind to more than one distinct site (*40*, *41*). We have also recently shown that the peptide GPRVVE, which is identical to the N-terminal sequence of the α-chain, can bind to both sites (*42*). The observation that "A:b" interactions can occur calls into question the model where only "A:a" interactions occur during thrombin- and batroxobin-catalyzed polymerization. The possibility that both "A:a" and "A:b" interactions occur upon the release of FpA may explain the observation that batroxobin-catalyzed polymerization proceeds quite normally. Perhaps "A:b" interactions, occurring intermittently, trigger the conformational changes usually brought about by "B:b" interactions. This possibility is supported by our recent studies with two variants with "b" site changes that prevented "B/b" interactions, Bβ D398A and Bβ E397A (*19*). Batroxobin-catalyzed polymerization of both Bβ D398A and Bβ E397A fibrinogens was impaired compared to that of normal recombinant fibrinogen. These biochemical data suggested that "A:b" interactions are part of batroxobin-catalyzed polymerization. This suggestion is supported by the structure presented here, showing GPRP in the "b" site in rfD-γD298,301A+GP, and the structure reported previously (*42*), with GPRVVE in the "b" site of normal fragment D (rfD-GPRVVE). Using similar reasoning, our data also indicate that "B:a" interactions are possible; therefore, the difference between batroxobin- and thrombin-catalyzed polymerization may arise from the addition of "B:a" interactions following the release of FpB. Further studies are clearly required to test these possibilities.

The conformation of the GHRP peptide bound to the "a" polymerization site in the rfD-γD298,301A+GH structure was unexpected. The unique conformation observed was first distinguished in a variant fibrinogen D fragment crystal, rfD-Bβ D398A+GH (pdb code 1RE3). In the 1RE3 structure, a unique conformation exists when GHRP is bound to the "a" polymerization site in an rfD molecule concurrent with calcium binding to the γ2 site. In the rfD-γD298,301A+GH structure, the crystal form is inconsistent with 1RE3, which would contain the packing-induced γ2 site and altered GHRP conformation. As expected, the rfD-γD298,301A+GH crystal data did not reveal calcium bound to the γ2 site; however, both molecules of the asymmetric unit exhibited the altered GHRP conformation. This result is comprehensible after considering the substitution and the resulting conformational

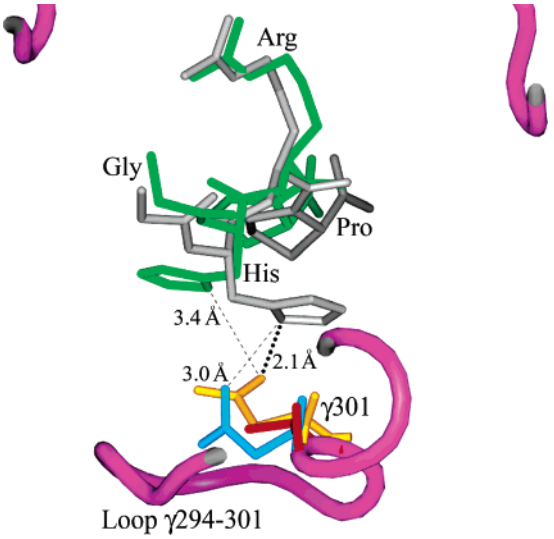

FIGURE 6: Steric limitations dictate GHRP's conformation in the "a" polymerization site. The environment of residue γ301 dictates the GHRP conformation because of the steric restraints that differ among the various structures. Shown is a top-down view of the "a" polymerization site with the γ-chain backbone colored in purple. The yellow γD301 side chain in normal fibrinogen (rfD-BOTH; 1LTJ) resides 3.4 Å from the His of the bound peptide shown in green. Both the γD301 side chain (blue) and GHRP (gray) alter their positions when the γ2 calcium-binding site is occupied (as in rfD-BβD398A+GH; 1RE3). The side chain of γA301 in the rfD-γD298,301A+GH structure is shown in red; in this structure, the peptide conformation is equivalent to that seen in 1RE3 (gray). Note that when the γD301 side chain from normal fibrinogen (yellow) is superimposed on the rfD-γD298,301A+GH structure (gray), there is a steric clash between the γD301 side chain and the His of GHRP (heavy dotted line), indicating the necessity of conformational flexibility in the peptide.

flexibility. The conformational flexibility of loop γ294−301 and the replacement of alanine at position γ301 both create more volume in the "a" polymerization site. The increased space provides the opportunity for GHRP to take on the alternate conformation that is presumed to be an energetically favorable conformation shown in Figure 6. By considering the point that steric concerns dictate the conformation of GHRP in the "a" polymerization site, we can infer the origin of the altered conformation concomitant with occupancy of the γ2 site. When the γ2 site is occupied by calcium, residue γD301 moves from pointing into the "a" polymerization site to an alternate position facing the bound calcium (Figure 6). This movement removes the steric hindrance of γD301 in the "a" site and allows the altered energetically favorable conformation. The replacement of γD301 with the smaller alanine residue similarly removes this steric hindrance; therefore, the His side chain can point into the polymerization pocket. These interpretations are supported by a recent publication that showed that the peptide AHRP binds selectively in the "b" site because of steric limitations in the "a" site (*43*).

ACKNOWLEDGMENT

We thank Dr. Matthew R. Redinbo (UNC-CH, Chapel Hill, NC) for his guidance during this project. We thank Dr. Laurie Betts for her technical suggestions, Dr. Brenda Temple at the UNC-CH Structural BioInformatics Core Facility (Chapel Hill, NC) for use of the computing facilities, the National Cell Culture Center for providing normal recombinant fibrinogen medium, and Dr. Zhongmin Jin at SER-CAT (Advanced Photon Source) for data collection. Use of the Advanced Photon Source was supported by the U.S. Department of Energy, Office of Science, Office of Basic Energy Sciences, under Contract No. W-31-109-End-38.

REFERENCES

1. Hall, C. E., and Slayter, H. S. (1959) The fibrinogen molecule: Its size, shape and mode of polymerization, *J. Biophys. Biochem. Cytol. 5*, 11−17.
2. Fowler, W. E., and Erickson, H. P. (1979) Trinodular structure of fibrinogen. Confirmation by both shadowing and negative stain electron microscopy, *J. Mol. Biol. 134*, 241−249.
3. Doolittle, R. F., Goldbaum, D. M., and Doolittle, L. R. (1978) Designation of sequences involved in the "coiled-coil" interdomainal connections in fibrinogen: constructions of an atomic scale model, *J. Mol. Biol. 120*, 311−325.
4. Veklich, Y. I., Gorkun, O. V., Medved, L. V., Nieuwenhuizen, W., and Weisel, J. W. (1993) Carboxyl-terminal portions of the alpha chains of fibrinogen and fibrin. Localization by electron microscopy and the effects of isolated alpha C fragments on polymerization, *J. Biol. Chem. 268*, 13577−13585.
5. Laudano, A. P., and Doolittle, R. F. (1978) Synthetic peptide derivatives that bind to fibrinogen and prevent the polymerization of fibrin monomers, *Proc. Natl. Acad. Sci. U.S.A. 75*, 3085−3089.
6. Olexa, S. A., and Budzynski, A. Z. (1980) Evidence for four different polymerization sites involved in human fibrin formation, *Proc. Natl. Acad. Sci. U.S.A. 77*, 1374−1378.
7. Laurent, T. C., and Blomback, B. (1958) On the significance of the release of two different peptides from fibrinogen during clotting, *Acta Chem. Scand. 12*, 1875−1877.
8. Hantgan, R. R., and Hermans, J. (1979) Assembly of fibrin. A light scattering study, *J. Biol. Chem. 254*, 11272−11281.
9. Weisel, J. W. (1986) Fibrin assembly. Lateral aggregation and the role of the two pairs of fibrinopeptides, *Biophys. J. 50*, 1079−1093.
10. Weisel, J. W., Veklich, Y., and Gorkun, O. (1993) The sequence of cleavage of fibrinopeptides from fibrinogen is important for protofibril formation and enhancement of lateral aggregation in fibrin clots, *J. Mol. Biol. 232*, 285−297.
11. Boyer, M. H., Shainoff, J. R., and Ratnoff, O. D. (1972) Acceleration of fibrin polymerization by calcium ions, *Blood 39*, 382−387.
12. Cooke, R. D. (1974) Calcium-induced dissociation of human plasma factor XIII and the appearance of catalytic activity, *Biochem. J. 141*, 683−691.
13. Dang, C. V., Bell, W. R., Ebert, R. F., and Starksen, N. F. (1985) Protective effect of divalent cations in the plasmin degradation of fibrinogen, *Arch. Biochem. Biophys. 238*, 452−457.
14. Everse, S. J., Spraggon, G., Veerapandian, L., and Doolittle, R. F. (1999) Conformational changes in fragments D and double-D from human fibrin(ogen) upon binding the peptide ligand Gly-His-Arg-Pro-amide, *Biochemistry 38*, 2941−2946.
15. Yee, V. C., Pratt, K. P., Cote, H. C., Trong, I. L., Chung, D. W., Davie, E. W., Stenkamp, R. E., and Teller, D. C. (1997) Crystal structure of a 30 kDa C-terminal fragment from the gamma chain of human fibrinogen, *Structure 5*, 125−138.
16. Spraggon, G., Everse, S. J., and Doolittle, R. F. (1997) Crystal structures of fragment D from human fibrinogen and its crosslinked counterpart from fibrin, *Nature 389*, 455−462.
17. Everse, S. J., Spraggon, G., Veerapandian, L., Riley, M., and Doolittle, R. F. (1998) Crystal structure of fragment double-D from human fibrin with two different bound ligands, *Biochemistry 37*, 8637−8642.
18. Kostelansky, M. S., Betts, L., Gorkun, O. V., and Lord, S. T. (2002) 2.8 Å crystal structures of recombinant fibrinogen fragment D with and without two peptide ligands: GHRP binding to the "b" site disrupts its nearby calcium-binding site, *Biochemistry 41*, 12124−12132.
19. Kostelansky, M. S., Bolliger-Stucki, B., Betts, L., Gorkun, O. V., and Lord, S. T. (2004) B beta Glu397 and B beta Asp398 but not B beta Asp432 are required for "B:b" interactions, *Biochemistry 43*, 2465−2474.
20. Kostelansky, M. S., Lounes, K. C., Ping, L. F., Dickerson, S. K., Gorkun, O. V., and Lord, S. T. (2004) Calcium-binding site beta

2, adjacent to the "b" polymerization site, modulates lateral aggregation of protofibrils during fibrin polymerization, *Biochemistry 43*, 2475−2483.
21. Doolittle, R. F., and Pandi, L. (2006) Binding of synthetic B knobs to fibrinogen changes the character of fibrin and inhibits its ability to activate tissue plasminogen activator and its destruction by plasmin, *Biochemistry 45*, 2657−2667.
22. Deutsch, D. G., and Mertz, E. T. (1970) Plasminogen: purification from human plasma by affinity chromatography, *Science 170*, 1095−1096.
23. Binnie, C. G., Hettasch, J. M., Strickland, E., and Lord, S. T. (1993) Characterization of purified recombinant fibrinogen: partial phosphorylation of fibrinopeptide A, *Biochemistry 32*, 107−113.
24. Deng, W. P., and Nickoloff, J. A. (1992) Site-directed mutagenesis of virtually any plasmid by eliminating a unique site, *Anal. Biochem. 200*, 81−88.
25. Lord, S. T., Strickland, E., and Jayjock, E. (1996) Strategy for recombinant multichain protein synthesis: fibrinogen B beta-chain variants as thrombin substrates, *Biochemistry 35*, 2342−2348.
26. Gorkun, O. V., Veklich, Y. I., Weisel, J. W., and Lord, S. T. (1997) The conversion of fibrinogen to fibrin: recombinant fibrinogen typifies plasma fibrinogen, *Blood 89*, 4407−4414.
27. Ng, A. S., Lewis, S. D., and Shafer, J. A. (1993) Quantifying thrombin-catalyzed release of fibrinopeptides from fibrinogen using high-performance liquid chromatography, *Methods Enzymol. 222*, 341−358.
28. Mullin, J. L., Gorkun, O. V., and Lord, S. T. (2000) Decreased lateral aggregation of a variant recombinant fibrinogen provides insight into the polymerization mechanism, *Biochemistry 39*, 9843−9849.
29. Furlan, M., Rupp, C., and Beck, E. A. (1983) Inhibition of fibrin polymerization by fragment d is affected by calcium, Gly-Pro-Arg and Gly-His-Arg, *Biochim. Biophys. Acta 742*, 25−32.
30. Solis, D., Arias, M., Tercero, J. C., and Diaz-Maurino, T. (1989) Fractionation of plasmic fibrin(ogen) digests by lectin affinity chromatography, *Thromb. Res. 55*, 221−232.
31. Otwinowski, Z., and Minor, W. (1997) Processing of X-ray diffraction data collected in oscillation mode, *Methods Enzymol. 276*, 307−326.
32. Brunger, A. T., Adams, P. D., Clore, G. M., DeLano, W. L., Gros, P., Grosse-Kunstleve, R. W., Jiang, J. S., Kuszewski, J., Nilges, M., Pannu, N. S., Read, R. J., Rice, L. M., Simonson, T., and Warren, G. L. (1998) Crystallography & NMR system: A new software suite for macromolecular structure determination, *Acta Crystallogr., Sect. D 54*, 905−921.
33. Brunger, A. T. (1993) Assessment of phase accuracy by cross validation—the free R-value—methods and applications, *Acta Crystallogr., Sect. D 49*, 24−36.
34. Jones, T. A., Zou, J. Y., Cowan, S. W., and Kjeldgaard, M. (1991) Improved methods for building protein models in electron-density maps and the location of errors in these models, *Acta Crystallogr., Sect. A 47*, 110−119.
35. Read, R. J. (1986) Improved Fourier Coefficients for Maps Using Phases From Partial Structures with Errors, *Acta Crystallogr., Sect. A 42*, 140−149.
36. Hurlet-Jensen, A., Cummins, H. Z., Nossel, H. L., and Liu, C. Y. (1982) Fibrin polymerization and release of fibrinopeptide B by thrombin, *Thromb. Res. 27*, 419−427.
37. Lewis, S. D., Shields, P. P., and Shafer, J. A. (1985) Characterization of the kinetic pathway for liberation of fibrinopeptides during assembly of fibrin, *J. Biol. Chem. 260*, 10192−10199.
38. Weisel, J. W., and Nagaswami, C. (1992) Computer modeling of fibrin polymerization kinetics correlated with electron microscope and turbidity observations: clot structure and assembly are kinetically controlled, *Biophys. J. 63*, 111−128.
39. Lounes, K. C., Ping, L., Gorkun, O. V., and Lord, S. T. (2002) Analysis of engineered fibrinogen variants suggests that an additional site mediates platelet aggregation and that "B-b" interactions have a role in protofibril formation, *Biochemistry 41*, 5291−5299.
40. Laudano, A. P., and Doolittle, R. F. (1980) Studies on synthetic peptides that bind to fibrinogen and prevent fibrin polymerization. Structural requirements, number of binding sites, and species differences, *Biochemistry 19*, 1013−1019.
41. Laudano, A. P., and Doolittle, R. F. (1981) Influence of calcium ion on the binding of fibrin amino terminal peptides to fibrinogen, *Science 212*, 457−459.
42. Betts, L., Merenbloom, B. K., and Lord, S. T. (2006) The structure of fibrinogen fragment D with the 'A' knob peptide GPRVVE, *J. Thromb. Haemostasis 4*, 1139−1141.
43. Doolittle, R. F., Chen, A., and Pandi, L. (2006) Differences in binding specificity for the homologous gamma- and beta-chain "holes" on fibrinogen: exclusive binding of Ala-His-Arg-Pro-amide by the beta-chain hole, *Biochemistry 45*, 13962−13969.

BI602607A